Available online at www.sciencedirect.com

SciVerse ScienceDirect

Advances in Space Research 51 (2013) 712–721

ADVANCES IN SPACE RESEARCH (a COSPAR publication)

www.elsevier.com/locate/asr

Total electron content of the ionosphere at two stations in East Africa during the 24–25 October 2011 geomagnetic storm

F.M. D'ujanga [a,*], P. Baki [b], J.O. Olwendo [c], B.F. Twinamasiko [a]

[a] Department of Physics, Makerere University, Kampala, Uganda
[b] Kenya Polytechnic University College, P.O. Box 52428, 00200 Nairobi, Kenya
[c] Pwani University College, P.O. Box 195, 80108 Kilifi, Kenya

Received 5 June 2012; received in revised form 26 September 2012; accepted 27 September 2012
Available online 6 October 2012

Abstract

The equatorial ionosphere has been known to become highly disturbed and thus rendering space-based navigation unreliable during space weather events, such as geomagnetic storms. Modern navigation systems, such as the Global Positioning System (GPS) use radio-wave signals that reflect from or propagate through the ionosphere as a means of determining range or distance. Such systems are vvulnerable to effects caused by geomagnetic storms, and their performance can be severely degraded. This paper analyses total electron content (TEC) and the corresponding GPS scintillations using two GPS SCINDA receivers located at Makerere University, Uganda (Lat: 0.3° N; Lon: 32.5° E) and at the University of Nairobi, Kenya (Lat: 1.3° S; Lon: 36.8° E), both in East Africa. The analysis shows that the scintillations actually correspond to plasma bubbles. The occurrence of plasma bubbles at one station was correlated with those at the other station by using observations from the same satellite. It was noted that some bubbles develop at one station and presumably "die off" before reaching the other station. The paper also discusses the effects of the geomagnetic storm of the 24–25 October 2011 on the ionospheric TEC at the two East African stations. Reductions in the diurnal TEC at the two stations during the period of the storm were observed and the TEC depletions observed during that period showed much deeper depletions than on the non-storm days. The effects during the storm have been attributed to the uplift of the ionospheric plasma, which was then transported away from this region by diffusion along magnetic field lines.

Keywords: Geomagnetic storm; Plasma bubbles; Uplifted plasma

1. Introduction

Corona mass ejections (CME) that enter the Earth's magnetic field may cause geomagnetic storms which usually occur in conjunction with ionospheric storms. CMEs are a result of solar wind outbursts from active parts of the sun. As the solar wind impinges on the magnetosphere, its velocity and pressure and its embedded interplanetary magnetic field (IMF) are highly variable due to its origin in different solar active regions. Sudden changes of its parameters, manifested as the occurrence of shock waves and most significantly the southward turning of the IMF Bz component, lead to a rapid increase of magnetic reconnection processes at the magnetopause. When Bz is strongly negative, magnetic reconnection between the IMF and the geomagnetic field produces open field lines which allow mass, energy and momentum to be transferred from the solar wind to the Earth's magnetosphere (Davis et al., 1997). This results in dramatic increase of solar wind energy input into all regions of the geosphere system, hence generating geomagnetic storms. A geomagnetic storm is usually defined by changes in the *Dst* (disturbance-storm time) index. The *Dst* index estimates the globally averaged change of the horizontal component of the Earth's magnetic field at the magnetic equator based on

* Corresponding author. Tel.: +256 772478333.
E-mail address: fdujanga@physics.mak.ac.ug (F.M. D'ujanga).

0273-1177/$36.00 © 2012 COSPAR. Published by Elsevier Ltd. All rights reserved.
http://dx.doi.org/10.1016/j.asr.2012.09.040

measurements from a few magnetometer stations. It is generally used for the definition of the different storm phases, as it marks the global activities during a geomagnetic storm. The *Kp* (planetary K) index, on the other hand, reflects the mid-latitude global magnetic activity and the north–south component of the IMF Bz controls the coupling of the solar wind to the magnetosphere. Geomagnetic activity generates energy inputs that generally take the form of enhanced electric fields, currents, and energetic particle precipitation and can significantly modify the ionosphere-thermosphere system (Migoya-Orue et al., 2009).

There are three distinctive geomagnetic storm phases: storm sudden commencement (SSC) phase, which is an impulse-like disturbance of the magnetic north component at mid- to high- latitude geomagnetic observatories caused by the first encounter of an interplanetary shock wave with the magnetosphere. The main storm phase is characterized by the build-up of the intensified ring current by high energetic particle injection and energization. This is connected with a decrease of the *Dst* values down to a minimum value which marks the end of the main phase and the beginning of the storm recovery phase. A magnetic storm main phase starts with a rapid decrease of *Dst*. Geomagnetic storm conditions prevail whenever *Dst* values are less than −50 nT and an actual global geomagnetic storm is an event with values between −50 nT and −100 nT and lasts for at least four consecutive hours (Forster and Jakowski, 2000). Most navigational and communication systems use radio-wave signals which reflect from or propagate through the ionosphere. The Global Positioning System (GPS), for example, uses radio signals that pass through the ionosphere and can be affected by space weather phenomena, and any changes in the electron density due to space weather activity can change the speed at which the radio waves travel, introducing a propagation delay in the GPS signal. Rapid changes in electron density resulting from space weather disturbances, such as geomagnetic storms, are associated with ionospheric scintillations which can have a great impact on GPS measurements, resulting in inaccurate positioning measurements. Rao et al. (2009), for example, reported loss of lock to a number of GPS receivers in the Indian region during a geomagnetic storm.

During a geomagnetic storm, the ionosphere can be modified in a complex and sometimes unpredictable manner. From recent studies (Rao et al., 2009; Basu et al., 2007), it is established that, in the longitude sectors where the main phase of the magnetic storm occurs during the local sunset hours, there is a greater probability of the storm induced electric fields to contribute to the increase in the eastward electric fields enhancing the post sunset vertical drifts at the equator. These vertical drifts may result in conditions whereby ionospheric plasma densities and electric fields develop irregular structures with scale lengths from hundreds of kilometers down to sub-meter sizes, a condition known as equatorial spread F (ESF). Plasma depletions, which are a manifestation of plasma bubbles, are the irregularities of the largest scale sizes (up to a few hundred km) that are associated with the ESF (Valladares et al., 2004; Dashora and Pandey, 2005). These plasma irregularities in the F region of the equatorial ionosphere manifest as diffused echoes on the ionograms and generally occur during nighttime and are observed (Tsunoda, 1980) to be aligned to Earth's magnetic field. The presence of plasma irregularities within these depletions disrupts communications and navigation systems by scattering radio wave signals that pass through them, a phenomenon known as ionospheric scintillation. The occurrence of these scintillations as satellite signals pass through the ionosphere is a clear indication of the fluctuations in the total electron content (TEC) of the ionosphere.

The origin and variability of the plasma density depletions in relation to the variability of ionospheric total electron content have been well documented (Valladares et al., 2004; Dashora and Pandey, 2005). Sudden reductions in TEC, observed in the nighttime low-latitude F-region, have been identified with the plasma density depletions of the equatorial origin (Valladares et al., 2004). TEC depletions occur when one or more plasma bubbles drift across the line-of-sight between the GPS receiver and the satellite. Also, rapid changes in electron density resulting from space weather disturbances may cause severe TEC depletions. During daytime, the E-region dynamo electric field gives rise to an upward electrodynamic $E \times B$ drift that causes the F-region plasma to diffuse downwards along geomagnetic field lines under the influence of gravity and pressure gradients, resulting into the equatorial ionization anomaly at about 15° magnetic latitude on either side of the equator. After sunset, plasma densities and dynamo electric fields in the E-region decrease, and the anomaly begins to fade, and at this local time a dynamo electric field develops in the F-region (Rao et al., 2006; Valladares et al., 2004). Polarization charges, set up by the conductivity gradients at the terminator, enhance the eastward electric field for about an hour after sunset. With the decreased ionization density in the E-region after sunset, vertical plasma density gradients form in the bottom side of the F-layer, resulting in the upward density gradients opposite in direction to the gravitational force. Such a configuration is known as the Rayleigh–Taylor (RT) instability, and allows plasma density irregularities to occur (Rao et al., 2006; Basu et al., 2007; Paznukhov et al., 2012). These irregularities can grow to become large ionospheric depletions, and are often referred to as equatorial plasma bubbles (EPBs).

This paper shows TEC values and GPS scintillations measured by two GPS SCINDA receivers located at Makerere University, Uganda (Lat: 0.3° N; Lon: 32.5° E) and at the University of Nairobi, Kenya (Lat: 1.3° S; Lon: 36.8° E), both in East Africa. These two stations are located close to the geographic equator and their geomagnetic coordinates are, respectively, Makerere (Lat. −9.3°; Lon. 104.2°) and Nairobi (Lat. −10.8°; Lon. 108.5°). By analyzing TEC depletions and the corresponding GPS scintillations, we are able to show that the scintillations actually correspond to plasma bubbles. We then try to correlate

the occurrence of the plasma bubbles at one station in relation to the other station. Finally, we discuss the effect of the 24–25 October 2011 magnetic storm on the ionospheric TEC at the two East African stations and show that the storm had an effect on the TEC depletions that occurred that day.

2. Experimental details

In this study, the ionospheric scintillations and total electron content (TEC) have been measured using high data-rate NovAtel GSV400B GPS SCINDA receivers situated at Makerere University, Uganda (Geomagnetic cords: Lat. -9.3^{o}; Lon. 104.2^{o}) and at the University of Nairobi, Kenya (Geomagnetic cords: Lat. -10.8^{o}; Lon. 108.5^{o}). From now on, in this paper, the Makerere University station will be denoted by Mak, and that at University of Nairobi by UoN. The GPS SCINDA is a real-time GPS data acquisition and ionospheric analysis system, and computes ionospheric parameters S_4 and TEC using the full temporal resolution of the receiver. The TEC is computed from the combined L1 (1575 MHz) and L2 (1228 MHz) pseudo ranges and carrier phase, and the scintillation index, S_4, is the statistical measure of the intensity of the amplitude scintillation of the L1 frequency (1575 MHz) GPS signals. The equipment is suited for studying several parameters simultaneously.

The ionospheric scintillations were monitored by computing the S_4 index, which is the fractional fluctuation of the signal due to ionospheric modulation. It is the standard deviation of the received signal power normalized to the average signal power, calculated for a one minute period based on a 50 Hz sampling rate (Carrano, 2007). The estimation of the absolute TEC using GPS receivers involves the leveling of the phases to pseudorange, in order to get the relative TEC; and the estimation or removal of instrumental biases (calibration), which gives the absolute TEC (Carrano and Groves, 2006). The total electron content is defined as the number of electrons in a column of 1 m^2 cross-section, from the height of the GPS satellite ($\sim$20,000 km) to the receiver on the ground, where *1 TEC unit* = 10^{16} *electrons*/m^2.

The scintillation index, S_4, and TEC data thus recorded, using the GPS receivers, are processed for each of the satellite passes with an elevation mask angle greater than 30^{o}, so that the effects of low elevation angles, such as tropospheric, water vapour scattering and multipath effects are avoided. At low elevation angles high S_4 index values are observed because the amplitude scintillation depends on the electron density deviations and on the thickness of the irregularity layer, both of which increase apparently at low elevation angles, causing stronger scintillations, and high S_4 index values due to multipath effects (Valladares et al., 2004; Groves and Carrano, 2009). The analysis of the scintillation and TEC data has been carried out using the Gopi GPS-TEC analysis application software, version 1.45, (Gopi, 2010). This program gives plots of vertical TEC on the screen and writes ASCII output files which are used for further analysis of the data.

3. Results and discussions

The results presented here are from the analysis of TEC values measured by two independent GPS receivers situated a distance of about 500 km apart and very close to the geographic equator, and located within the equatorial anomaly region. By analyzing TEC depletions at the two stations during the year 2011, ionospheric plasma bubbles have been identified and monitored between the two stations, as discussed in Section 3.1. In Section 3.2, an attempt has been made to show that the geomagnetic storm of 24–25 October 2011 had an effect on the diurnal TEC and on the occurrence of ionospheric TEC depletions.

3.1. TEC depletions

Sudden reductions in TEC, observed in the nighttime low-latitude F-region, have been identified as plasma density depletions of the equatorial origin. For a reduction in TEC to be considered a depletion, it must be followed by a recovery to a level near the TEC value preceding the depletion (Valladares et al., 2004). It is important to note this because there may be other non-bubble-related processes that could produce quick reductions in the TEC value, and lead to a mistaken identification of the TEC depletions. A TEC depletion occurs when one or more plasma bubbles drift across the line-of-sight between the GPS receiver and the satellite. TEC depletions are considered a manifestation of the equatorial plasma bubbles. During solar maximum, equatorial F-region irregularities are found to occur in the early evening hours, developing over the magnetic equator and extending in both horizontal and vertical directions (DasGupta et al., 2007). These bubbles are upwelled by the electrodynamic ExB drift over the magnetic equator and map down to the off-equatorial locations along magnetic field lines. As the bubbles move, normally from west-to-east across a satellite link, ionization depletions and scintillations are usually encountered (Dashora and Pandey, 2005; DasGupta et al., 2007; Seemala and Valladares, 2011). It has been observed that during such strong depletions and scintillation, deep amplitude fades or large phase fluctuations may cause signal disruptions in the receiver- satellite link (Skone and de Jong, 2000; Rao et al., 2009).

This section presents results for TEC depletions detected in the month of April 2011 at the two stations labeled Mak for the Uganda station and UoN for the Kenya station. Same days have been chosen for comparison in order to assess the longitudinal extension of the plasma bubbles over a distance of 500 km in East Africa. In recent studies plasma density depletions of the equatorial origin have been identified in this region for the year 2010 (D'ujanga et al., 2012), for March 2011 (Olwendo et al., 2012) and over the African region for 2010 (Paznukhov et al.,

2012). In the current research, many more depletions were detected within this region owing to the fact that 2011 is in the ascending solar activity period. The month of April 2011, has been chosen particularly for this research since it happened to have moderately quiet geomagnetic conditions as seen from the *Dst* plot in Fig. 3b. This will then form a good comparison with the conditions that prevailed during the geomagnetic storm of 24–25 October 2011, discussed in Section 3.2. The results presented will be for a particular satellite designated by a pseudorandom number (PRN). The cases selected in this research are those when the satellite was overhead at both stations, since such an elevation will provide a TEC depletion width almost equal to the true bubble cross section (Valladares et al., 2004). This is also good for comparison purposes and, in addition, the signals would not suffer from multipath reflections, as is the case for low elevation angles. The horizontal axis of each panel corresponds to the universal time (UT) and the corresponding local time can be obtained by adding 3 h to UT. For each plot of TEC variation, there is a corresponding S_4 index displayed below it to assess the level of scintillation. Values of the S_4 index which are lower than 0.2 were considered insufficient to give a significant level of scintillation.

Fig. 1a shows TEC depletions measured at the two sites, on 1 April 2011, at Makerere University, denoted as Mak (Geomagnetic latitude MLAT: -9.3^{o}) and at the University of Nairobi, denoted as UoN (MLAT: -10.8^{o}) using signals from PRN 26 GPS satellite. It will be assumed for all cases that the plasma depletions are traversing a quasi-stationary receiver-satellite link, due to the relatively slow east–west motion of the GPS satellites (Valladares et al., 2004). The TEC plot shows a series of depletions at Mak that started at 17:50 UT and ended at 20:10 UT, while those at UoN started just a little earlier at 17:45 UT and ended at 20:00 UT. If we assume that we are looking at the same bubble which is moving in the west-to-east direction, then it appears that the onset of the plasma depletions started at UoN (in the east) rather than at Mak. This apparent anomaly can be explained if the bubbles were allowed to tilt westward at altitudes above the F-region peak. The westward tilt will make the part

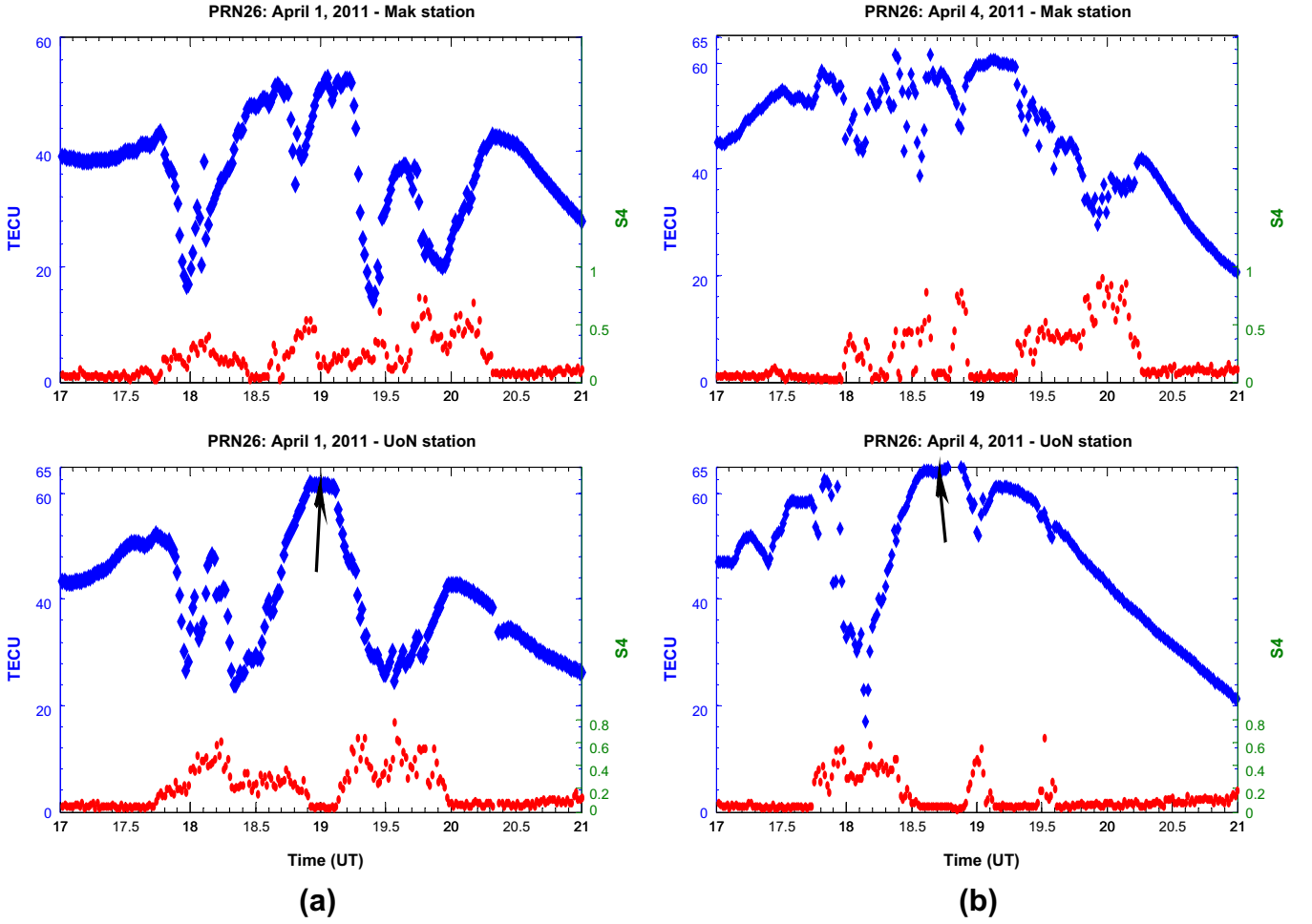

Fig. 1. TEC depletions observed with PRN26 satellite with the corresponding S_4 index below shown with round (red) markers. (a) Shows the plots for 1 April 2011 at Mak station (top-panel) and at UoN station (bottom-panel). (b) Shows the plots for 4 April 2011 at Mak (top-panel) and at UoN (bottom-panel). We can observe that the S_4 index corresponds to the depletions in TEC. Most notably is the absence of depletions, and hence scintillations, at the UoN station on both days (indicated by arrow), while there are depletions at the Mak station with corresponding scintillations. (For interpretation of the references to color in this figure legend, the reader is referred to the web version of this article.)

of the TEC depletions that extends to higher latitudes to appear at slightly later times (Valladares et al., 2004). This may be the most probable reason why the depletions at UoN seem to have started earlier than those at Mak in the west. The GPS scintillations, indicated by the S_4 index, correspond with the TEC depletions. They both show high S_4 index values ranging from 0.2 to well over 0.7. The Makerere station shows a TEC depletion of about 10 TECU, which occurred between 18h40 and 19h00 UT, and triggered a scintillation of index of about 0.6, with no corresponding depletion at the Nairobi station. This may imply that the bubble that was seen at Makerere started developing between the two stations and presumably "died off" before it could be detected by the Nairobi station.

Fig. 1b shows depletions at the same locations as in Fig. 1a and sighted by PRN 26, on 4 April 2011. The depletion registered at about 18:10 UT, is recorded by both stations. The Mak station shows a very small depletion giving a corresponding S_4 index of 0.4, while UoN station shows a much larger depletion which triggers a scintillation index of about 0.6. From the onset of the scintillations, it appears the UoN station registers the depletion before the Mak station. After that depletion, the station at UoN registers another TEC depletion at about 19h00 of magnitude 10 TECU, and the Mak station registers the same. However, between these two, the Mak station registers other small depletions, which trigger S_4 index of up to 0.8., while nothing is registered at the UoN station, depicting another case where bubbles presumably "die off" between the two stations.

From the two cases analyzed above, 1 April 2011 and 4 April 2011, we note that the depletions show that these GPS scintillations correspond to plasma bubbles or depletions in the equatorial F-region (Valladares et al., 2004). It is further noted that these bubbles are tilted in altitude that is why the station that is about 500 km east registered the bubble occurrence slightly earlier than the station in the west (Valladares et al., 2004). Finally, we note that there are some bubbles that develop at one station and presumably "die off" before reaching the other station.

3.2. The geomagnetic storm of 25 October 2011

The analysis of TEC data can help demystify complex behavior of competing interactive processes during ionospheric storms just as a number of studies have indicated (Jakowski et al., 1999; Rao et al., 2009; Basu et al., 2007). Electric fields, thermospheric meridional winds, a composition bulge and high latitude particle precipitation have been suggested as probable physical mechanisms to explain the ionospheric reaction to geomagnetic storms observed at different latitudes (Basu et al., 2007; Fuller-Rowell et al., 1994; Mahrous, 2007, and references therein). During the geomagnetic disturbance there is an input of energy into the polar ionosphere, which changes several thermospheric parameters, such as composition, temperature and circulation. Composition changes directly influence the electron concentration in the F2 region, and hence the TEC, while circulation spreads the heated gas to lower latitudes. It has been reported (Basu et al., 2007) that during major magnetic storms the currents associated with inner magnetospheric electric field directed in the dusk-to-dawn direction are no longer able to shield the mid-latitude and equatorial latitudes from high-latitude electric fields. This results in instantaneous penetration of electric fields from high latitude to the middle and the equatorial ionosphere. The conflict between the storm-induced circulation and the regular circulation determines the spatial distribution of the negative and positive phases.

TEC observations were made for the year 2011, which registered a number of mild geomagnetic storms, but 24–25 October 2011 registered a storm with $Dst = -137$ nT and $Kp = 6$. The previous months of August and September 2011 were characterized by a number of mild storms, with sub-major ones occurring on 6 August 2011 and 26 September 2011, with minimum Dst values of -113 nT and -103 nT, respectively. The geomagnetic storm that occurred on 24–25 October 2011, was a major disturbance as shown by the geomagnetic perturbation indices Kp, Dst and IMF Bz, plotted in Fig. 2. This storm had been preceded by a storm sudden commencement (SSC) event

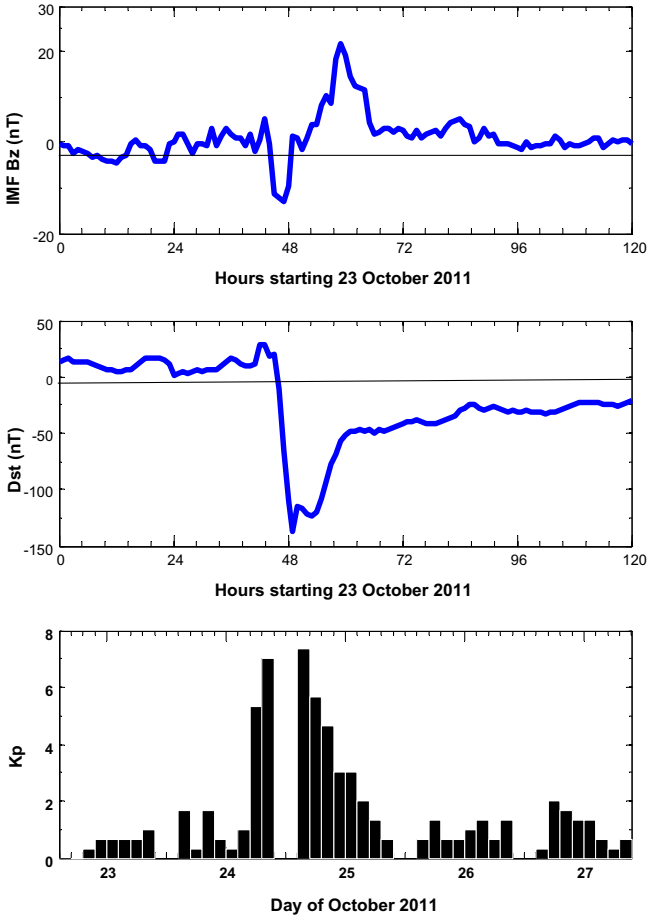

Fig. 2. Geomagnetic indices during 24–25 October 2011. Top-panel: IMF Bz component of solar wind (from ACE data); middle-panel: Dst index of geomagnetic activity (from noaa); bottom panel: Kp index.

registered at 17h00 UT on 24 October 2011. The IMF Bz turned sharply southward at 19h00 UT on 24 October 2011, and attained a maximum negative value of −12.9 nT at 23h00 UT. It can be seen from Fig. 2 that the *Kp* index started rising before the southward turning of IMF Bz, was still high even when the IMF Bz changed direction, and it decayed more slowly than it rose. To some extent, this reflects the fact that *Kp* index is correlated with the southward turning of the IMF (Davis et al., 1997).

Dst index was at an average value of about 12 nT prior to the southward turning. Before the time of the southward turning, there was the SSC, immediately after which point it decreased rapidly to a minimum value of −137 nT. This represents a significant enhancement of the ring current (Basu et al., 2007; Forster and Jakowski, 2000). Even after 72 h (3 days) after the commencement of the storm, *Dst* still did not recover to the initial value and remained at about −25 nT, though the storm is deemed to have ended when the *Dst* is −50 nT. The positive phase just before the commencement of the storm at 19h00 indicate that the field is compressed, implying that the factors generating the positive phase have a bearing on the southward turning of the IMF (Davis et al., 1997; Burton et al., 1975). The *Dst* index decreased sharply after 21h00 UT on 24 October 2011, and attained its maximum negative value of −137 nT at 01h00 UT on 25 October 2011 giving a decrease rate of about 40 nT/h. Basu et al. (2007) reported that when a sudden intensification of the ring current occurs leading to *Dst* decreases at such large rates, the electric field penetration from high latitudes causes the formation of ionospheric irregularities of electron density in the mid-latitude and the equatorial region. For the present study, a CME occurred on 24 October 2011 at 18h00 UT and was reported by the Goddard Space Weather Laboratory analyst to have caused a strong compression of Earth's magnetic field, allowing solar wind to penetrate all the way down to the geosynchronous orbit for a brief period between 19h06 UT and 19h11 UT on the same day (www.spaceweather.com). This CME could have contributed to the occurrence of the geomagnetic storm on 24–25 October 2011.

3.2.1. Variation of diurnal TEC during the geomagnetic storm

The diurnal variation of TEC during the geomagnetic storm period of 23–27 October 2011 has been compared with the diurnal variation of TEC for the seemingly quiet

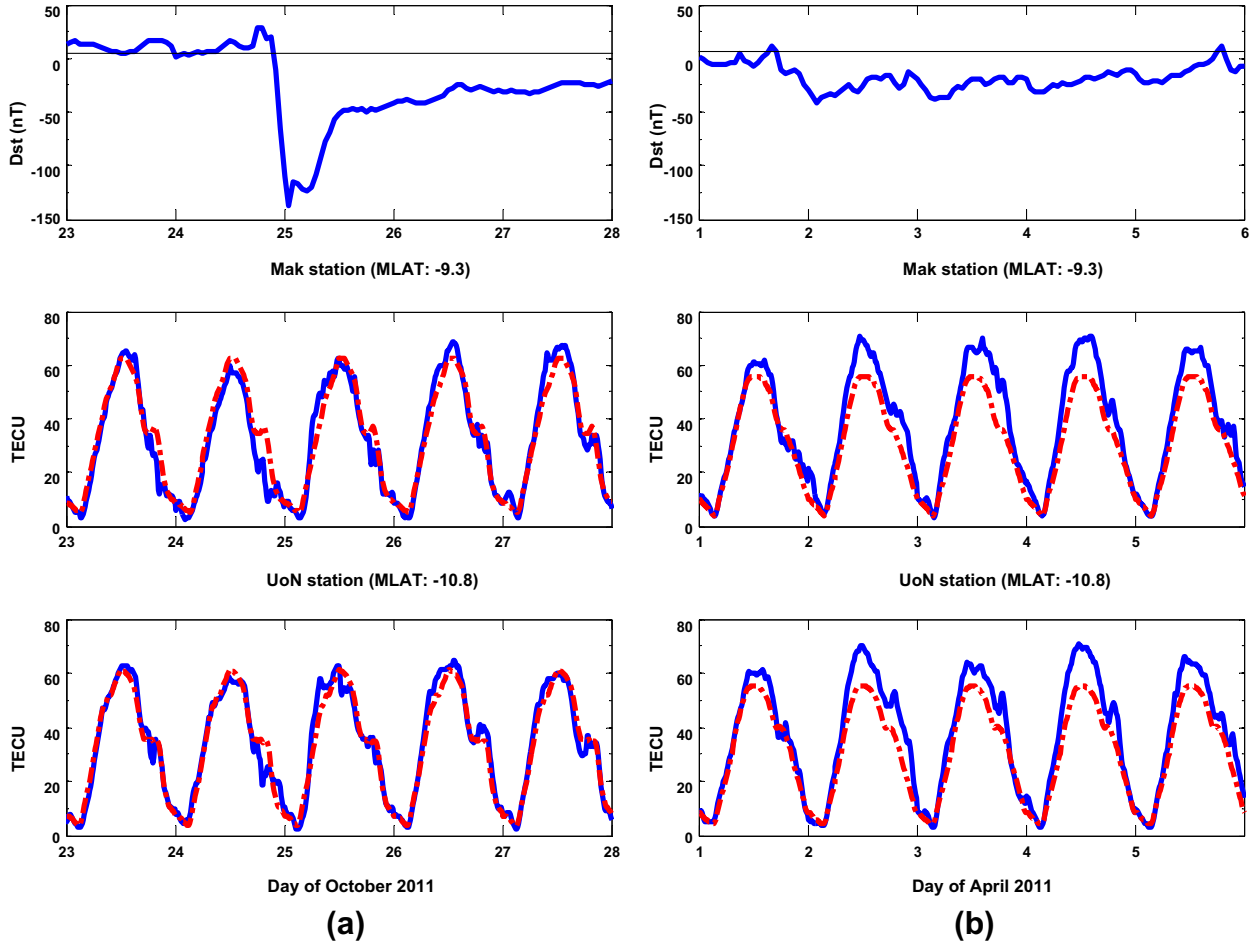

Fig. 3. The diurnal variation of TEC: (a) Depicts the period of the geomagnetic storm of 24–25 October 2011, with the Mak station in the middle-panel and the UoN station in the bottom-panel. (b) Depicts the seemingly quiet period in April 2011, with the Mak station in the middle-panel and the UoN station in the bottom-panel. In both cases, the *Dst* index for that period is presented in the top panels.

period of 1–5 April 2011 for the two stations in this study, as shown in Fig. 3. The *Dst* indices for the corresponding periods are also shown in the same figure. The diurnal variation of TEC is compared with the monthly mean for each month, shown by the dashed (red) line. It can be seen that on the day(s) of storm, 24–25 October, there was a depression in the vertical TEC, i.e. it was less than the monthly mean TEC, except for the short period during the storm recovery segment (before noon on 25 October 2012). This could be due to the wave-like perturbations depicted in Fig. 3c and discussed in the last paragraph of this section. However, before and after the storm, the daily values are generally higher than the monthly mean, just as is the case for the seemingly quiet period of 1–5 April 2011, shown in Fig. 3b. This situation is the same at the two stations in this study, which are near the geographic equator, with MLAT of -9.3^{o} and -10.8^{o}, respectively. Such a decrease in TEC at equatorial stations was reported by Rao et al. (2009), when they presented TEC of stations in a region covering the equatorial to the anomaly crest regions and beyond in the Indian sector. The TEC was low at the equatorial station, increased gradually to the stations within the crest anomaly and then started decreasing significantly beyond the crest. This behavior was attributed to the redistribution of ionization associated with the storm induced effects which differ from the equator to the anomaly crest regions owing to the dynamic changes of the ionosphere over the low latitude regions.

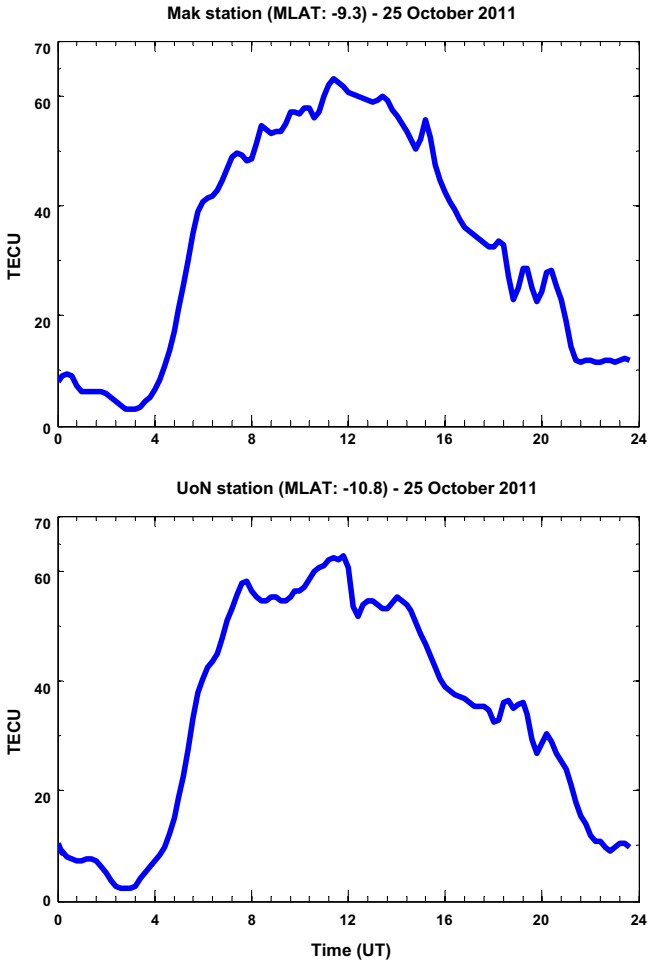

Fig. 3c. The wave-like perturbations in the diurnal TEC between 8 h and 15 h UT on 25 October 2011, during the recovery phase of the storm. The top-panel depicts the Mak station and the bottom-panel depicts the UoN station.

As mentioned above concerning Fig. 2 the IMF Bz turned sharply southward at 19h00 UT on 24 October 2011, and attained a maximum negative value of −12.9 nT at 23h00 UT. On occasions, when the IMF Bz remains southward for several hours and the magnetic activity continues to intensify, the penetration of the electric field into the low-latitude ionosphere may persist for many hours as reported by Basu et al. (2007). Other studies (Migoya-Orue et al., 2009) have shown an increase of vertical TEC at the equatorial anomaly crests during geomagnetic storms in comparison to pre-storm conditions. Foster and Coster (2007) observed an increase of TEC at and pole-ward of the crests of the equatorial anomalies which they attributed to plasma uplift and redistribution from low- to mid-latitudes. Also observed was the variation of TEC at the magnetic equator, in the region of the South American anomaly (10^{o} S, 320^{o} E), where vertical TEC dropped sharply. It is proposed that in addition to an eastward electric field needed to uplift and destabilize the low-latitude ionosphere and enhance and spread the equatorial anomaly peaks, a pole-ward electric field component is needed to account for the significant buildup of TEC pole-ward of the crests of the anomaly, as observed in these events. Thus, the decrease of TEC at the two East African stations on the days of the storm indicates that there could have been plasma uplift due to eastward penetration electric field; and in such a case, the bottom side of the ionosphere presumably lifted and the uplifted plasma was transported away from this region along magnetic field lines (Basu et al., 2007; Foster and Coster, 2007; Rao et al., 2009). Such plasma structures, in an environment of high plasma density, such as the equatorial region, may cause intense phase and amplitude scintillations of satellite signals and thereby adversely impact satellite communication and navigation systems.

The diurnal variation of TEC depicted significant fluctuations in TEC at the two stations, which started during the recovery phase of the storm. The fluctuations lasted for about 5 h, from 10h00 to 15h00 UT as shown in Fig. 3c. Such wave-like perturbations in diurnal TEC during geomagnetic storms have also been reported in the Indian sector (Rao et al., 2009) and in the South American region (Basu et al., 2007). It was proposed that storm shocks might have induced wave-like perturbations in TEC, indicating the presence of gravity wave type perturbations in the ionosphere. Such perturbations could be due to the prompt penetration of high-latitude electric fields to lower latitudes, as discussed above. It goes on further to confirm that the effect of the eastward electric field penetration on

the ionosphere at these stations during the SSC phase of the storm persisted throughout the recovery phase of the storm.

3.2.2. Effect of the storm on TEC depletions

The geomagnetic storm that occurred on 24–25 October 2011 had its effects also depicted in the ionospheric TEC depletions that occurred on those two days. The GPS data for the two nights shows large depletions in TEC with correspondingly large scintillation indices. Fig. 4 shows plots of TEC and S_4 index for the two stations on the two nights of the storm Fig. 4a displays the TEC and S_4 index plots at the Mak (Uganda) station in the upper panel and at the UoN (Kenya) station in the bottom panel on 24 October 2011. Severe depletions in TEC can be observed at both stations with values going below 10 TECU. These depletions occurred before the onset of the geomagnetic storm. However, the conditions that preceded the storm could have had a bearing on the behavior of TEC and the depletions therein. The positive phase just before the commencement of the storm at 19h00 on 24 October 2011 showed that the field was compressed, implying that the factors that generated the positive phase had a bearing on the southward turning of the IMF (Davis et al., 1997; Burton et al., 1975). The southward turning of IMF Bz observed during the initial commencement of the storm must have given rise to the prompt penetration electric field of magnetospheric origin, which is known to produce remarkable effects in the equatorial ionosphere as the $E \times B$ plasma drift becomes severely affected (Basu et al., 2007; Huang et al., 2010; Swisdak et al., 2006; Rao et al., 2009). Thus, such electric fields will make the equatorial F-region plasma drift upwards in the daytime and downwards in the nighttime. Under normal circumstances, the zonal field in the equatorial F-region is eastward during the daytime and is westward during the nighttime. The penetration electric fields associated with the southward turning of the IMF Bz are, therefore, so directed as to enhance the effective electric fields and the associated drifts at the equator. Therefore, the large depletions in TEC detected at these two East African stations indicates that the plasma was uplifted due to eastward penetration electric fields, and that

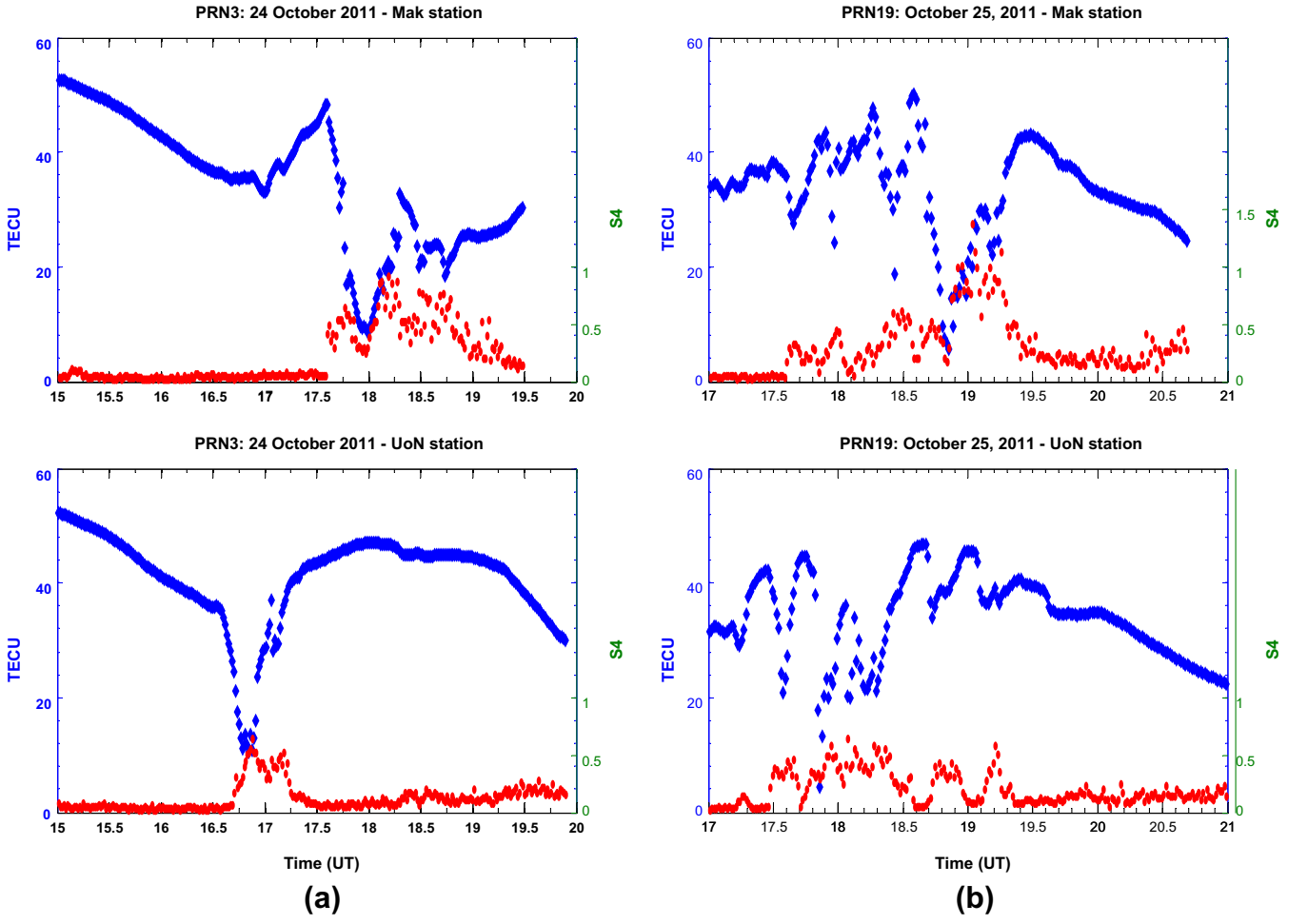

Fig. 4. TEC depletions observed by GPS satellites during the storm period of 24–25 October 2011, with the corresponding S_4 index below shown with round (red) markers. (a) Shows the plots for PRN3 on 24 October 2011 at Mak station (top-panel) and at UoN station (bottom-panel). (b) Shows the plots for PRN19 on 25 October 2011 at Mak (top-panel) and at UoN (bottom-panel). Large depletions with TEC values less than 10 TECU can be observed at both stations.

the plasma was then transport away from the region presumably by diffusion along magnetic field lines (Basu et al., 2007).

Fig. 4b displays the GPS data at the two stations on 25 October 2011, some 17–20 h after the commencement of the storm. The top panel shows TEC and S_4 plots for the Mak station, and the bottom panel shows the plots for the UoN station. High scintillation values of S_4 index ranging from 0.6 to 1.4 can be observed at both stations and very large depletions in TEC can also be detected at both stations. Of particular mention is the depletion at Mak showing a depletion of 6.6 TECU and that at UoN showing a depletion 4.5 TECU. It must be pointed out, however, that the year 2011 registered quite a high number of depletions in TEC at these two stations, but the geomagnetic storm in question brought out severe depletions. These can be compared with the depletions in Fig. 1 which occurred on 'normal' days. The deep depletions seen on this day also go onto emphasize the point that during the geomagnetic storm, there was plasma uplift due to eastward penetration electric field and plasma transport away from the region presumably by diffusion along magnetic field lines.

4. Conclusions

Total electron content (TEC) and the corresponding GPS scintillations have been analyzed using two independent GPS SCINDA receivers located a distance of 500 km apart within East Africa. The analysis shows that the scintillations correspond to plasma bubbles of equatorial origin, which are tilted westward at altitudes above the F-region peak. The occurrence of some of these bubbles at one station and not the other was evidence that some bubbles can develop at one station and presumably "die off" before reaching the other station. During the storm period of 24–25 October 2011, there was a significant decrease in the diurnal variation of TEC at both stations. It was further noted that the diurnal variation of TEC depicted significant fluctuations in TEC at the two stations, which started during the recovery phase of the storm, on 25 October 2011 and lasted for about 5 h. The geomagnetic storm could have induced wave-like perturbations in TEC, indicating the presence of gravity wave type perturbations in the ionosphere. It further goes on to confirm that the effects during the SSC phase of the storm persisted throughout the recovery phase of the storm. Another notable effect of the geomagnetic storm was the large depletions in TEC detected at these two East African stations during the storm period. The TEC values dropped to less than 10 TECU.

Furthermore, there was the southward turning of IMF Bz observed during the initial commencement of the storm which sharply dropped to -137 nT., suggesting the presence of the prompt penetration electric fields of magnetospheric origin. Generally, the prompt penetration electric field of magnetospheric origin, characterized by southward turning of IMF Bz, produces a dawn-dusk electric field which is eastward during the daysides and westward in the nightsides in the equatorial ionosphere. These prompt penetration fields produce remarkable effects in the equatorial ionosphere as the $E \times B$ plasma drift is severely affected. Thus, such electric fields will make the equatorial F-region plasma drift upwards in the daytime and downwards in the nighttime. Under normal circumstances, the zonal field in the equatorial F-region is eastward during the daytime and is westward during the nighttime. The penetration electric fields associated with the southward turning of the IMF Bz are, therefore, so directed as to enhance the effective electric fields and the associated drifts at the equator.

Therefore, the effects observed in TEC during the geomagnetic storm of 24–25 October 2011, notably the reduction in the diurnal TEC, the wave-like perturbations in the diurnal TEC and the large TEC depletions, indicate that that there could have been plasma uplift due to eastward penetration electric fields; and in such a case, the bottom side of the ionosphere presumably lifted and the uplifted plasma was transported away from this region along magnetic field lines. Such plasma structures, in an environment of high plasma density, such as the equatorial region, may cause intense phase and amplitude scintillations of satellite signals and thereby adversely impact satellite communication and navigation systems.

Acknowledgements

The authors would like to extend their gratitude to Boston College and the Air Force Research Laboratory (AFRL), USA, who supplied the GPS receivers used at the two stations in this research. The corresponding author would like, in a special way, to thank the Physics Department at the University of Nairobi for the offer of office space and access to all laboratory facilities while on sabbatical leave at the institution.

References

Basu, S., Basu, S., Rich, F.J., Groves, K.M., MacKenzie, E., Coker, C., Sahai, Y., Fagundes, P.R., Guedes, F.B. Response of the equatorial ionosphere at dusk to penetration electric fields during intense magnetic storms. J. Geophys. Res. 112, A08308, 2007.

Burton, R.K., McPherron, R.L., Russell, C.T. An empirical relationship between interplanetary conditions and Dst (Abstract). J. Geophys. Res. 80, 4204–4214, 1975.

Carrano, C.S., Groves, K. The GPS segment of the AFRL-SCINDA global network and the challenges of real-time TEC in the Equatorial Ionosphere. ION NTM, Montery, CA, pp. 1036–1047, 2006.

Carrano, C.S. GPS-SCINDA: A real-time GPS data acquisition and ionospheric analysis system for Scinda. Atmosph. & Environ. Res., Inc., GPS-SCINDA, 2007.

D'ujanga, F.M., Mubiru, J., Twinamasiko, B.F., Basalirwa, C., Ssenyonga, T.J. Total electron content variations in equatorial anomaly region. Adv. Space Res., http://dx.doi.org/10.1016/j.asr.2012.05.005, 2012.

DasGupta, A., Paul, A., Das, A. Ionospheric total electron content (TEC) studies with GPS in the equatorial region. Ind. J. Radio Space Phys. 36, 278–292, 2007.

Dashora, N., Pandey, R. Observations in equatorial anomaly region of total electron content enhancements and depletions. Ann. Geophys. 23, 2449–2456, 2005.

Davis, C.J., Wild, M.N., Lockwood, M., Tulunay, Y.K. Ionospheric and geomagnetic responses to changes in IMF *BZ*: a superposed epoch study. Ann. Geophys. 15, 217–230, 1997.

Forster, M., Jakowski, N. Geomagnetic effects on the topside ionosphere and plasmasphere: a compact tutorial. Surv. Geophys. 21, 47–87, 2000.

Foster, J.C., Coster, A.J. Conjugate localized enhancement of total electron content at low latitudes in the American sector. J. Atmos. Solar Terres. Phys. 69, 1241–1252, 2007.

Fuller-Rowell, T.J., Codrescu, M.V., Moffett, R.J., Quegan, S. Response of the thermosphere and ionosphere to geomagnetic storms. J. Geophys. Res. 99, 3893–3914, 1994.

Gopi, S. Rinex GPS-TEC program, version 1.45. Boston College, 2010.

Groves, K., Carrano, C. Scintillation impact on GPS. Satellite Navig. Sci and Tech for Africa Workshop (23rd March – 9th April 2009, ICTP, Trieste, Italy).

Huang, C.M., Chen, M.Q., Liu, J.Y. Ionospheric positive storm phases at the magnetic equator close to sunset. J. Geophys. Res. 115, A07315, 2010.

Jakowski, N., Schluter, S., Sardon, E. Total electron content of the ionosphere during the geomagnetic storm on 10th January 1997. J. Atmos. & Solar Terres. Phys. 61 (299–307), 1999.

Mahrous, A. Global Ionospheric Response to the Magnetic Storm of 21 October 1999. Austr. J. Basic & Appl. Sci. 1 (4), 678–686, 2007.

Olwendo, J.O., Cilliers, P.J., Baki, P., Mito, C. Using GPS-SCINDA observations to study the correlation between scintillation, total electron content enhancement and depletions over the Kenyan region. Adv. Space Res. 49, 1363–1372, 2012.

Orue, M.Y.O., Radicella, S.M., Coisson, P. Low latitude ionospheric effects of major geomagnetic storms observed using TOPEX TEC data. Ann. Geophys. 27, 3133–3139, 2009.

Paznukhov, V.V., Carrano, C.S., Groves, K.M., Caton, R.G., Valladares, C.E., Semaala, G.K., Bridgwood, C.T., Adeniyi, J., Amaeshi, L.L.N., Damtie, B., D'ujanga, F.M., Ndeda, J.O.H., Baki, P., Obrou, O.K., Okere, B.K., Tsidu, G.M. Equatorial plasma bubbles and L-band scintillations in Africa. Ann. Geophys. 30, 675–682, 2012.

Rao, P.V.S.R., Krishna, S.G., Niranjan, K., Prasad, D.S.V.V.D. Study of spatial and temporal characteristics of L-band scintillations over the Indian low-latitude region and their possible effects on GPS navigation. Ann. Geophys., 24, 1567–1580, 2006.

Rao, P.V.S.R., Krishna, S.G., Prasad, J.V., Prasad, S.N.V.S., Prasad, D.S.V.V.D, Niranjan, K. Geomagnetic storm effects on GPS based navigation. Ann. Geophys. 27, 2101–2110, 2009.

Seemala, G.K., Valladares, C.E. Statistics of total electron content depletions observed over the South American continent for the year 2008. Radio Sci. 46, 2011, doi: http://dx.doi.org/10.1029/2011RS004722.

Skone, S., de Jong, M. The impact of geomagnetic substorms on GPS receiver performance. Earth Planets Space 52, 1067–1071, 2000.

Swisdak, M., Huba, J.D., Joyce, G., Huang, C.S. Simulation study of a positive ionospheric storm phase observed at Millstone Hill. Geophys. Res. Lett. 33, L02104, 2006.

Tsunoda, R.T. Magnetic-field-aligned characteristics of plasma bubbles in the nighttime equatorial ionosphere. J. Atmos. Terr. Phys. 42, 743–752, 1980.

Valladares, C.E., Villalobos, J., Sheehan, R., Hagan, M.P. Latitudinal extensions of low-latitude scintillations measured with a network of GPS receivers. Ann. Geophys. 22, 3155–3175, 2004.